SPACE TELESCOPE SCIENCE INSTITUTE
Operated for NASA by AURA

Instrument Science Report WFC3 2004-11

WFC3 UVIS Crosstalk Images

S.Baggett, G.Hartig (STScI), E.Cheung (Jackson & Tull/GSFC)
July 9, 2004

ABSTRACT

This report summarizes the behavior of the Wide Field Camera 3 UVIS channel crosstalk features seen in the first ground-test data from the integrated instrument. There appear to be two types of crosstalk: the first arises from sources at any exposure level (from a few DN up to saturation); the crosstalk from a source in one amp appears in the three other amps as mirror images of the source. The second type arises from highly saturated pixels only; in these cases, the crosstalk appears in the adjoining amp of the same CCD as the source. Both types of crosstalk are highly nonlinear, occur at very low levels (<10DN/ pixel at the default gain of 1.5), and depend upon the bias level, gain, and pixel binning settings. A software workaround to eliminate some of the crosstalk is currently in hand in the form of timing patterns with alternate clamp times. The hardware cause for some of the crosstalk, a common-mode noise susceptibility in the CCD electronics box, has been identified and successfully fixed in the non-flight hardware; the problem is expected to be fixed in the flight hardware later this year. Meanwhile, further tests are underway at the Detector Characterization Lab (DCL at GSFC) to explore additional possible causes of crosstalk in the camera head electronics.

Introduction

WFC3 has been undergoing integration and testing at the GSFC (Goddard Space Flight Center), in the SSDIF (Space Systems Development and Integration Facility) clean room. In Dec2003-Jan 2004, an abbreviated science calibration test, or “mini-cal”, of the UVIS channel in the integrated instrument was performed. This was the first opportunity to test the full UVIS system and verify end-to-end instrument performance; ISR 2004-02 (Reid, 2004) presents a summary of the tests and calibration results. Images taken during the

mini-calibration, of a simulated point source in the WFC3 field of view, showed low level electronic mirror images, or crosstalk, of the source appearing in other amp(s).

The WFC3 crosstalk features were not entirely unexpected, as crosstalk can occur whenever two or more channels are read out simultaneously (Janesick, 2001). Furthermore, the WFC3 CEB (CCD electronics box) design is based upon that for the ACS (Advanced Camera for Surveys) and ACS data has shown low-level crosstalk between its four CCD quadrants (ACS April 2004 STAN). As reported in the ACS newsletter, the ACS WFC crosstalk features can be positive or negative, and are always at a low level, typically less than ~2DN/pixel (default gain of 1) . No crosstalk is seen in the ACS HRC channel since the chip is read out through only one amplifier.

This report summarizes the behavior of the WFC3 UVIS crosstalk features, the results from the crosstalk-related tests performed during the mini-calibration, and the mitigation plans.

Data

All images taken during the “mini-cal” that were useful for the crosstalk investigation are tabulated in Appendix A. The table lists images taken during tests specifically designed to investigate the WFC3 crosstalk behavior as well as images taken for other purposes (e.g., throughput measurements) which were useful for the crosstalk investigation. The following sections present the results from these image sets, including the behavior of the crosstalk in standard unbinned images and in other types of image readouts, the effect on the crosstalk of parameters such as the CCD bias offset level and/or the gain, in both the source and victim quadrants, and the effect of alternate timing patterns.

Crosstalk in standard, unbinned, full-frame, four-amp readout

Figure 1 presents the WFC3 crosstalk features in an inverted extreme log stretch of a full-frame, four-amp, gain 1.5, unbinned readout of a highly-saturated point source (HeNe laser in the optical stimulus) placed in the D quadrant center. Expected optical ghosts appear in quadrant A (‘figure 8’ ghost, due to reflections from the CCD surface and the inner detector window). A more extended, out of focus ghost (resulting from reflection between the detector windows and the filter) is visible in quadrants B/D, which in this particular type of image does not produce any crosstalk. Positive mirror images, or crosstalk, of the interior of the PSF are readily apparent in quadrants A,B,C while negative crosstalk of the the ‘figure 8’ optical ghost can be seen quadrants B,C, and D. The small number of negative crosstalk columns in quadrant C seem to be a second type of crosstalk, to be dis-

cussed more in later sections; the columns are a mirror image of only the heavily saturated pixels and appear only in the same chip as the source.

Figure 1: Crosstalk features due to a saturated PSF and its optical ghost are visible as the small circular spots in the center of quads A,B,C and the figure-8's in quads B,C,D. The saturated PSF is in quad D, optical ghosts are in quads A and B/D. The image is a gain 1.5, full-frame unbinned four-amp readout, and has been displayed with an extreme hard log inverted stretch in order to highlight the crosstalk features.

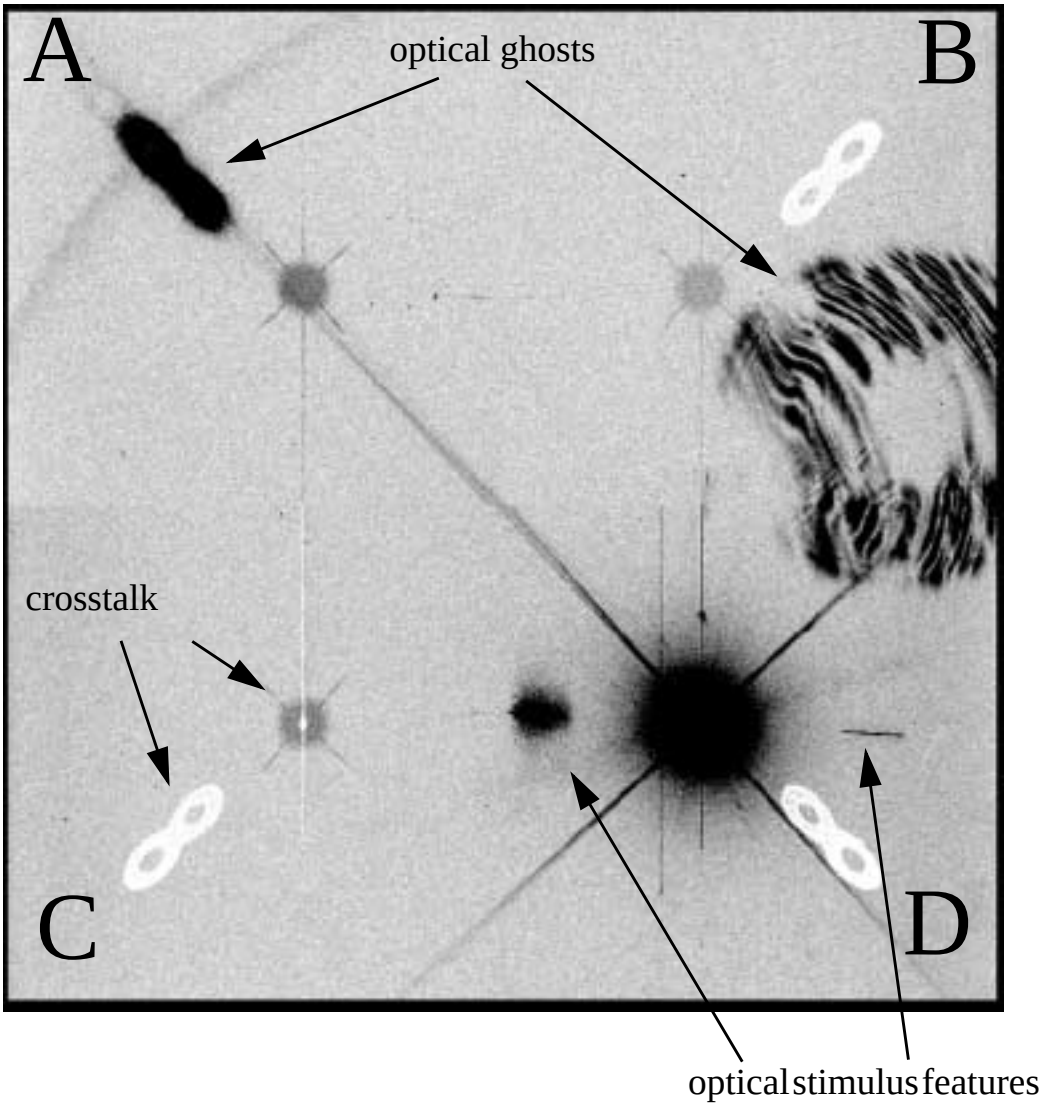

The behavior of the crosstalk is highly non-linear and does not scale with source counts. Figure 2, for example, shows average crosstalk levels due to the PSF and the optical ghost from Figure 1. The highly saturated PSF in quadrant D produces crosstalk in quadrants A,B,C at the 1-3 DN level (with the crosstalk type 2 appearing as -3DN trough). On the other hand, the optical ghost in quadrant A, with an exposure level of only ~150 DN, produces crosstalk at an average level of -3 to -1DN in quadrants B,C, and D. Though they did in this particular case, it should be noted that low source levels do not necessarily result in negative mirror images.

Figure 2: Averages of 20 rows taken through the PSF (top row of plots) and optical ghost (bottom row), with corresponding crosstalk levels overplotted.

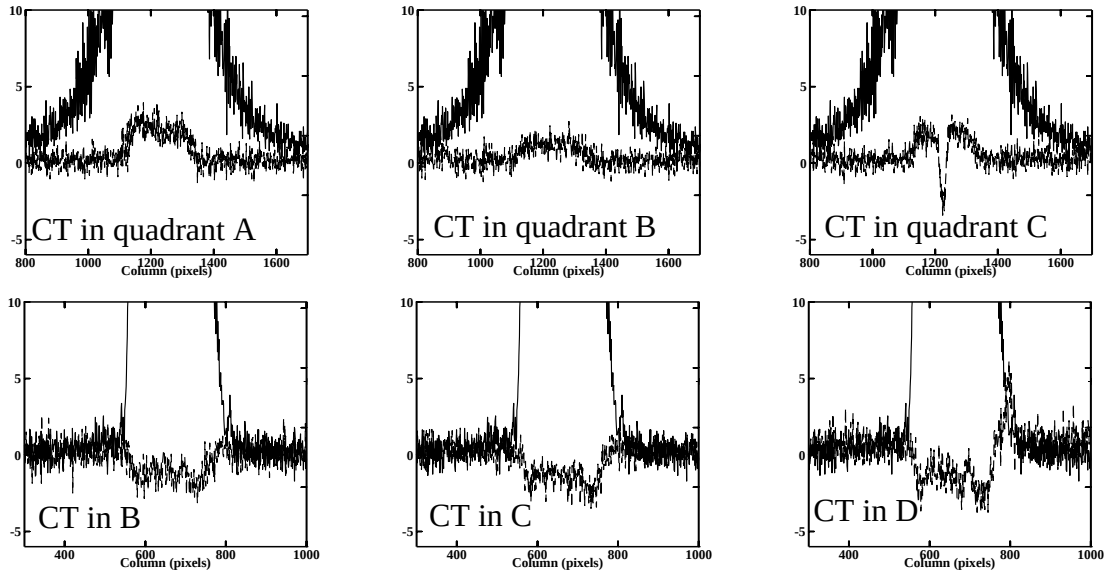

As seen in Figure 2, the magnitude of the crosstalk is ~1-3DN on average; a closer look, as in Figure 3, shows that individual crosstalk pixels can range up to a maximum of -10DN to +10DN. Figure 3 presents the count levels of source pixels plotted against the count levels seen in the mirrored crosstalk pixels; the left figure shows pixels from the PSF in quadrant D and its corresponding crosstalk pixels in quadrant A while the right figure shows pixels from the optical ghost in A and its corresponding crosstalk pixels in quadrant B. Crosstalk pixels in other quadrants show similar, highly-non-linear behavior: individual crosstalk pixels have count levels up to -10 to +10DN maximum and all levels in between, while the source pixels range from near 0 to more than 50,000DN.

Figure 3: Source pixel count levels plotted as a function of corresponding crosstalk pixel count levels, from a gain 1.5, full-frame four-amp readout image. The left plot shows pixel levels from a subsection of the PSF in qudarant D versus the level in the mirrored crosstalk pixels in quadrant A while the right plot shows pixels levels from a subsection of the optical ghost in quadrant A versus levels in its corresponding crosstalk pixels in quadrant B. For statistics, see Table 2, row 4 and row 16.

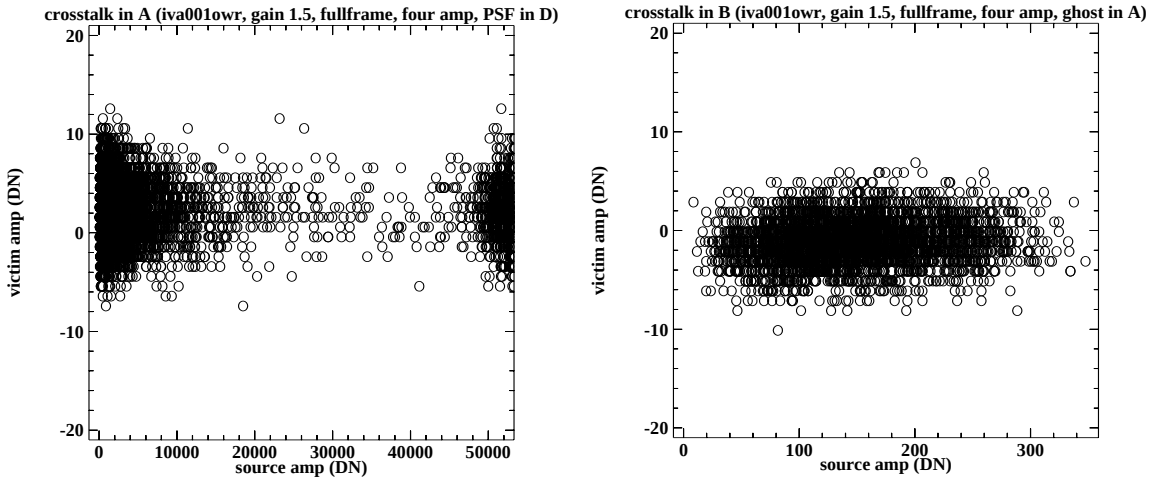

Crosstalk behavior in other types of standard readouts

The previous section presented the crosstalk features due to an input PSF and its associated optical ghosts in a standard, default gain (1.5), unbinned, full-frame, four-amp readout. WFC3 has the capability of performing image readouts using other combinations of amps (at least two amps are required for full-frame readouts). In Table 1 below, we summarize the location of crosstalk features in images taken with these other types of readouts, with and without on-chip binning. For these tests, the PSF was always placed in quadrant D and the optical ghost in question appeared in quadrant A, the same configuration used for the image in Figure 1.

As can be seen in Table 1, the two-amp, binned readouts show no detectable crosstalk of any type. These sorts of readouts, however, are not a viable workaround to the crosstalk issue as they have double the clamp time - which in full-frame readouts doubles the readout overhead time. Also apparent from Table 1 is that the binned, four-amp readouts have considerably less crosstalk. For exposures with the target placed in quadrant D, the crosstalk of the PSF appears consistently only in quadrant C and mirrors only the highly saturated pixels in quadrant D. This single-quadrant (single chip) crosstalk is most likely

caused by a different electronic problem than the multi-quadrant crosstalk. It is not believed to be produced in the on-chip circuitry, since it was not observed during the chip-level testing using non-flight electronics in the GSFC DCL. The ACS, which employs entirely different CCDs (from Scientific Imaging Technologies, or SITe) and a somewhat different pre-amp design, does not exhibit this type 2 crosstalk.
Additional binned images were taken with the PSF placed in the quadrant A, B, and C, confirming that these generated crosstalk type 2 only in quadrants B, A, and D, respectively (e.g., images 1573, 1579, 1587 in Appendix A). Figure 4 shows two binned images: a four-amp readout on the left, where the saturated pixels in quadrant D give rise to crosstalk type 2 in quadrant C and a two-amp readout on the right, where no crosstalk of either type could be found.

Table 1. Location of crosstalk features in standard readout images. Listed are the quadrants containing crosstalk of the PSF, C(P), and crosstalk of the A-quadrant optical ghost, C(G). All images had the saturated PSF placed in quadrant D; the optical ghost appeared in quadrant A.

Readout Amps	**ABCD**	**AD**	**BC**	**AC**	**BD**
no binning	C(P): ABC C(G): BCD	C(P): A C(G): D	C(P): A C(G): D	C(P): B C(G): C	C(P): B C(G): C
2x2 binning	C(P): C	None	None	None	None
3x3 binning	C(P): C	None	None	None	None

Figure 4: On the left is an example of a binned, full-frame, four-amp readout image; the type 2 crosstalk in quadrant C remains, due to saturated pixels in quadrant D. On the right is an example of a binned, full-frame, two-amp readout image; no crosstalk of any type is apparent.

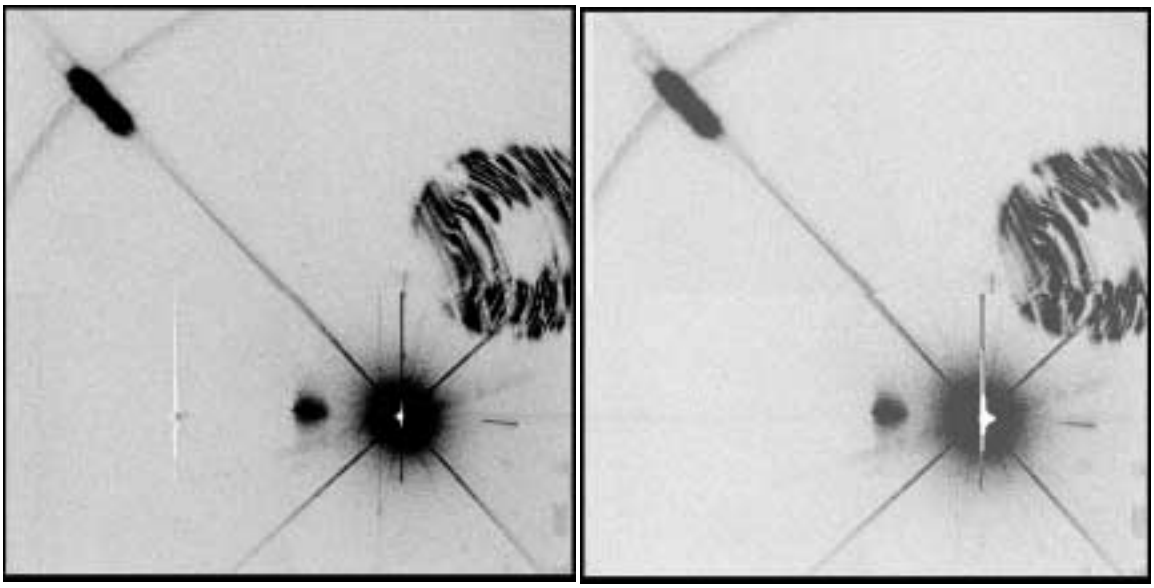

Effect of bias offset level changes

Special commanding was used in some of the ground test images to adjust the bias offset level (on-orbit, the bias offset will not be a parameter adjustable by the observer). These images showed that in all amps, changes in the bias level can result in dramatic changes in the crosstalk features. Figure 5, illustrates the crosstalk behavior in a series of gain 1.5 images taken with different bias levels, from the maximum down to the minimum pedestal. The crosstalk of the A-quadrant optical ghost can be seen to change from negative to positive to ringlike then back to positive depending upon the bias pedestal offset setting while the PSF crosstalk ranges from positive, to nearly non-existent, to ringlike. In any given image, the crosstalk in all amps appear similar (whether positive, negative, or ringlike). The average crosstalk level is typically between 0.5 to 2.5 DN: one area of the PSF crosstalk was at ~2.5DN level in the offset 0 image and ~1DN in the offset 6 image; at offset 3, the edges of the crosstalk are at ~2.5DN while the center is well below 0.5DN. The large optical ghost in quadrants B/D (at a level of a few 10's of DN) does not show crosstalk except at bias offset 2 (~3300 DN pedestal).

Figure 5: Crosstalk changes due to bias offset level settings; gain was kept at 1.5 throughout. Top row images, from left to right, have bias offset levels of 0 (4750DN, same as in Figure 1), 1 (4000DN) and 2 (3300DN) while bottom row images have offset levels of 3 (2600DN) and 6 (345DN).

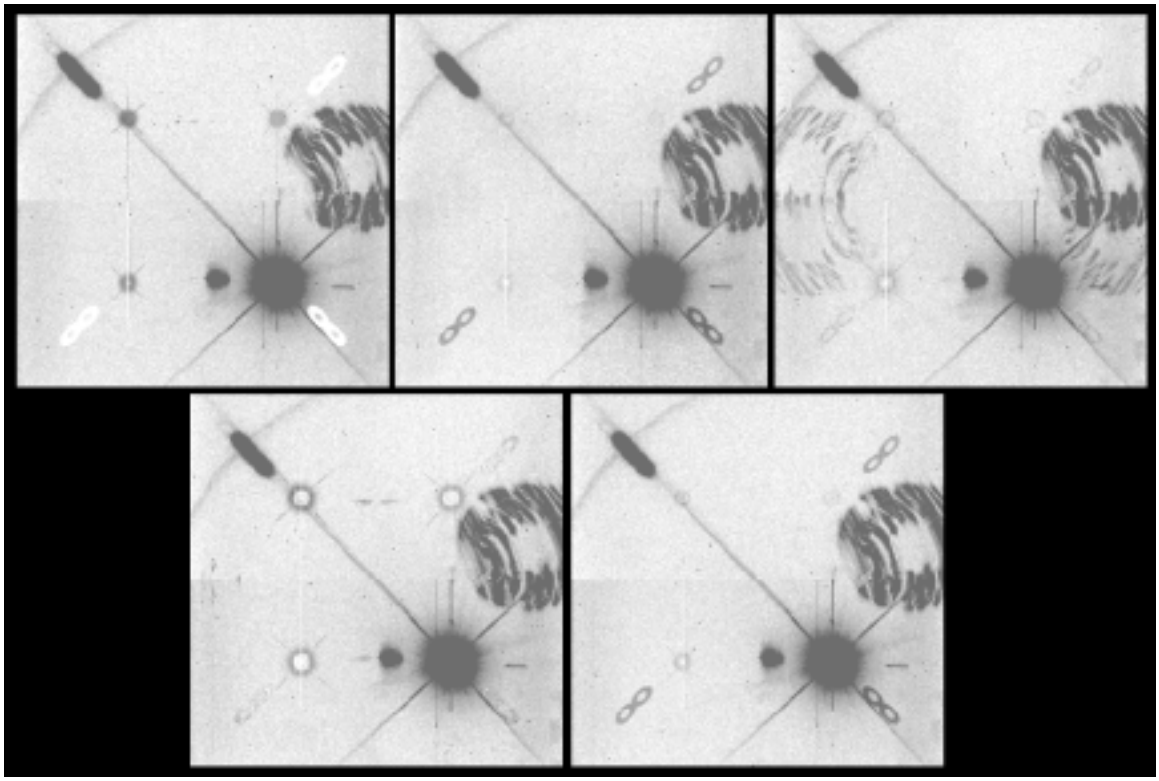

Additional tests were run, changing the bias in one amp only while leaving all the other amps at the nominal bias level. Bias offset level changes to only the source amp dramatically change the nature of the crosstalk while changing the bias offset level in the victim amp only has no significant effect on the crosstalk.

Effect of gain changes

Though only one default gain (1.5) is planned to be offered to general observers, the WFC3 instrument is capable of operating at three other gains (1.0, 2.0, and 4.0). In the ground tests of the WFC3 crosstalk, the various gain levels were exercised and found to dramatically change the character of the crosstalk, implying that the crosstalk-inducing signal occurs somewhere within or following the gain stage. Figure 6 shows four unbinned, full-frame, four-amp readout images taken at the four gains; both the character and sign of the crosstalk features are radically different, depending upon the gain setting. Even the low-level optical ghost in quadrants B/D produces crosstalk at certain gains: a mix of negative and positive features at gain=1 and solely positive features at gain=4.

Figure 6: Changes in crosstalk due to gain, using a hard stretch (+/- 3DN) to highlight the features: the PSF crosstalk changes sign while the large ghost crosstalk is transient.

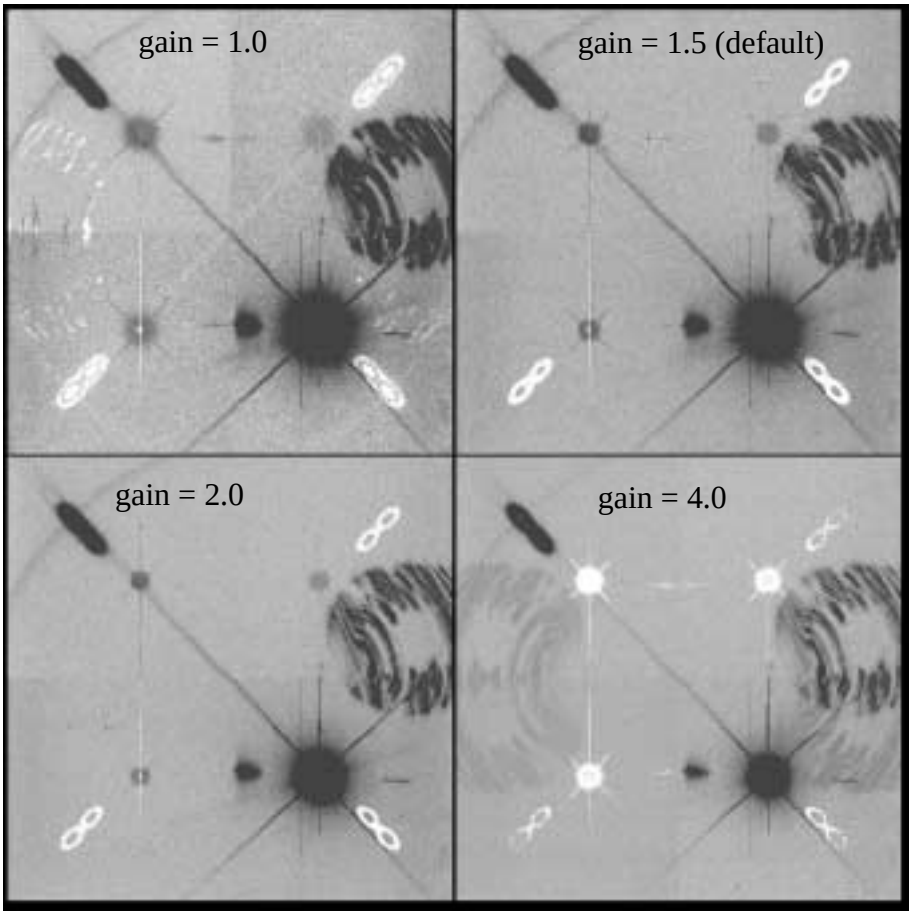

Table 2 lists the statistics of a subset of source pixels and their corresponding crosstalk pixels in each victim amp; the regions sampled are the same as those upon which Figure 3 (gain 1.5) was based. Generally, the average crosstalk due to the PSF in quadrant D appears slightly higher in quadrant A than other quadrants; the average crosstalk due to the low-level optical ghost in quadrant A is slightly higher in quadrant D than other quadrants. Occasionally, the average crosstalk seems to scale with gain (e.g., crosstalk in quadrant A has a mean of 1.5DN at gain 1 and 2.3DN at gain 1.5), however, in many cases it does not scale linearly (e.g., quadrant A has a mean of 1.5DN at gain 1 and a mean of 1.8 DN at gain 4). The average crosstalk levels are typically at the 1-4 electron level but individual pixels can exhibit crosstalk up to 10-15 electrons at the default gain. Overall, the crosstalk at the lower gain setting appears to be slightly weaker than at the default gain of 1.5. The higher gain settings appear to have slightly higher average crosstalk levels, in contrast to the ACS images, where the crosstalk was seen to be somewhat weaker at the higher gain setting (ACS April 2004 STAN).

To close out the gain investigations, special commanding was used to take some images where the gain was changed in some amps while holding the other amps at the default gain. Changing the gain in only the source amp once again dramatically changes the crosstalk features in the other (victim) amps. For example, the crosstalk feature is a positive mirror image at one gain setting and negative at another gain setting or the feature has a plateau-like shape at one gain and a ring shape at another gain setting. Though the crosstalk features change with the gain setting, on average they do not change in a linear fashion (e.g., images 3318, 3321). For example, the crosstalk in one pair of images averaged ~1.9DN at gain 1.5 but only 1.1DN at gain 4; another pair of images showed crosstalk at the 2.4DN level at gain 1.5 but 1.4 DN at gain 4.

In contrast to the bias offset level, changing the gain in only the crosstalk (victim) amp also changes the crosstalk behavior. Once again, the crosstalk features can appear dramatically different (e.g., plateau-like or ringlike, images 3315, 3316); average crosstalk count levels are about 1-3DN in magnitude.

Table 2. Statistics of source pixel count levels and their corresponding crosstalk pixel count levels in each victim amp, for a representative subsection of the PSF (first half of table) and one of the optical ghosts (last half of table).

		source pixels						crosstalk pixels				
gain	**npixels**	**mean**	**stddev**	**median**	**min**	**max**	**amp**	**mean**	**stddev**	**median**	**min**	**max**
1.0	10201	10880.6	20052.0	1757.4	62.4	60755.4	A	1.5	4.2	1.7	-15.3	18.7
							B	0.7	3.4	0.7	-12.3	13.7
							C	0.4	4.0	0.3	-14.7	12.3
1.5	10201	8711.5	17099.8	1192.4	36.4	53503.4	A	2.3	2.7	2.6	-7.4	12.6
							B	1.2	2.4	0.9	-8.1	9.9
							C	1.2	2.8	1.6	-9.4	10.6
2.0	10201	6248.7	12246.9	832.9	37.9	38310.9	A	1.8	2.1	2.1	-5.9	9.1
							B	0.9	1.8	1.0	-6.0	8.0
							C	1.0	2.1	1.6	-7.4	7.6
4.0	10201	3095.8	6005.8	418.8	12.8	18665.8	A	-1.5	1.6	-1.4	-6.4	3.6
							B	-0.9	1.3	-0.5	-5.5	4.5
							C	-1.0	1.5	-1.3	-8.3	4.7
1.0	3416	221.6	94.3	215.2	14.7	540.7	B	-0.5	3.2	-0.4	-11.4	12.6
							C	-0.6	3.2	-0.7	-11.7	10.3
							D	-0.4	3.5	-0.7	-13.7	11.3
1.5	3416	147.6	61.5	141.6	8.6	347.6	B	-1.1	2.3	-1.1	-10.1	6.9
							C	-1.2	2.2	-1.4	-9.4	6.6
							D	-1.3	2.5	-1.6	-10.6	7.4
2.0	3416	104.8	44.1	101.1	7.1	238.1	B	-0.9	1.9	-1.0	-7.0	6.0
							C	-1.0	2.0	-1.4	-7.4	5.6
							D	-1.2	2.3	-1.1	-8.1	6.9
4.0	3416	50.5	20.3	49.7	4.7	115.7	B	-0.7	1.4	-0.5	-5.5	4.5
							C	-0.6	1.5	-0.3	-5.3	4.7
							D	-1.3	2.1	-1.2	-7.2	4.8

Crosstalk behavior in non-standard readouts, via timing pattern changes

Some images were taken with custom-designed timing patterns, changing the default timing pattern clamp times in increments of 1 μs while keeping the total readout time fixed (it is highly desirable to minimize any increase in readout time, in order to minimize the total overhead time required for each exposure thereby maximizing observing efficiency). A suite of images were taken with clamp time offsets of -4,-3, -2... up to +7μs from the nominal 11 μs clamp time. The clamp is used to set the reference level for the pixel being read out, after which the signal is sampled and held, then sent through the ADC for conversion to DN. The clamp time sweep test was performed initially at the gain 4 setting (where the default timing pattern yielded the most prominent crosstalk) and then repeated at the default gain 1.5 setting.

Figure 7 shows a hard stretch of quadrant C for each of these different timing patterns at gain 1.5; in the absence of crosstalk, this quadrant would appear blank. The crosstalk is quite prominent in the -3μs offset pattern, less prominent in the -2μs offset pattern. The noise is about the same for the -1μs offset and the nominal patterns, but rises sharply in those patterns with positive clamp time offsets. The plot in Figure 8 shows the noise levels, measured from the image overscan regions, in the gain 1.5 images as a function of clamp time offset. The +6μs offset pattern timing pattern yields the lowest amount of crosstalk but the noise is higher. The -2μs offset pattern provides the best combination of low crosstalk and low noise. The crosstalk remaining in the -2μs offset pattern is at the same average level as in the nominal pattern: ~2-3 DN.

Figure 7: Hard stretch (+/-3DN) showing the crosstalk reaction to small changes to the nominal 11μs clamp time. Images show quadrant C crosstalk only (see Figure 1) and were all taken at the default gain of 1.5. The upper row shows the patterns with -4, -3, -2, -1μs clamp time offsets from the nominal clamp time; middle row shows the patterns with 0, +1, +2, +3μs clamp time offsets from nominal and lower row shows the +4, +5, +6, +7μs offsets from nominal.

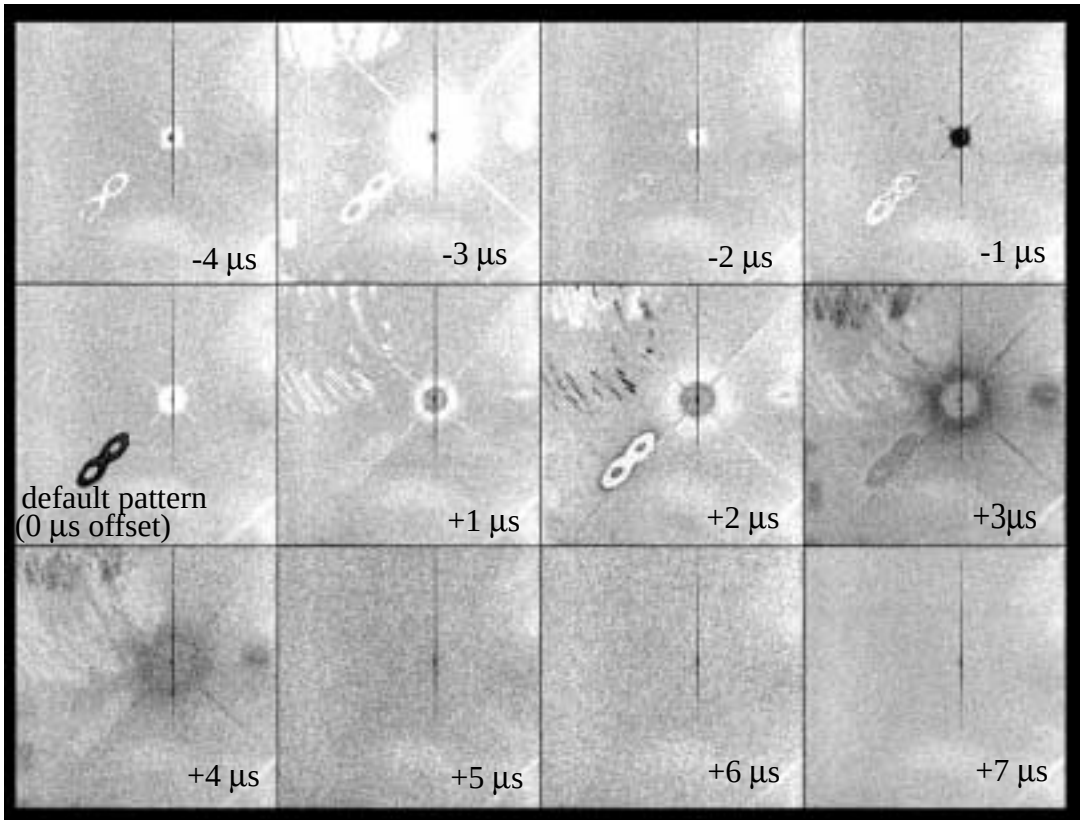

Figure 8: Noise as a function of clamp time offset.

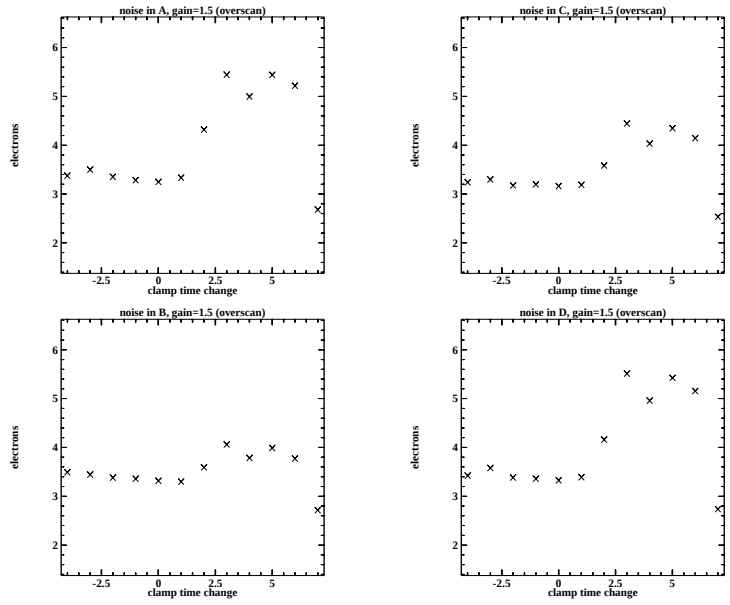

For completeness, we mention here that in the gain 4 timing pattern sweep, the +6µs pattern removed all the multi-amp crosstalk, leaving only the relatively minor saturated-pixel crosstalk (Figure 9 in Appendix B) ; the noise however, was 1-3 e^- worse than in the nominal timing pattern. In the case of gain 4, the -3µs pattern provided the smallest amount of crosstalk while keeping the noise at about the same level as in the nominal pattern.

Results from non-flight CEB

Although changing the timing pattern reduces the crosstalk and provides a software workaround with the cost of a slight increase in noise, it does not address the fundamental cause of the crosstalk. The engineering team at GSFC and Ball investigated the crosstalk problem on the non-flight CEB, using oscilloscope traces (imaging checks were not possible). Crosstalk similar to that seen from point sources in the WFC3 could be reproduced but crosstalk seen in extended sources was not reproducible. Close examination of the schematics of the CEB circuitry showed a possibility of a common-mode susceptibility in the 1Mhz frequency band. This suspicion which was confirmed by using a SPICE (Simulation Program with Integrated Circuit Emphasis) simulation. Once an appropriate capacitor was added to rebalance the front-end of the analog signal processing in the CEB, the crosstalk virtually disappeared from the traces. This fix conclusively identifies the reason for the crosstalk in the CEB; it has not yet been installed on the flight hardware, remaining a lien item to be implemented at a later time.

If the SPICE analysis is correct, a similar common-mode problem is also present in the pre-amp of the UVIS camera head. WFC3 has a somewhat different pre-amp design than ACS, which may be why the crosstalk appears to be slightly worse than it is in ACS. Possible pre-amp problems are currently being investigated in the DCL at GSFC, using the modified non-flight CEB in conjunction with the surrogate detector, with the intent to fix the problem in the hardware if at all possible.

Conclusions

The integrated WFC3 UVIS channel exhibits low-level crosstalk features, similar to but more pronounced than those seen in ACS. There are two types of crosstalk: the first arises from pixels at any exposure level and appears as mirror images in all amps while the second is due to heavily saturated pixels and appears in the alternate amp of the source CCD only. Both types of crosstalk are extremely nonlinear and highly gain- and bias level offset-dependent. Changes in the bias level of the source amp and changes in the gain of the source and/or victim amps change the sign, shape, and/or magnitude of the crosstalk features. Changes to the bias level of the victim amp appear to have no effect on the crosstalk.

Binning full-frame four-amp readouts has been shown to remove the type 1 crosstalk while binning full-frame two-amp readouts completely removes both types of crosstalk. Aside from being binned, these types of readouts also have twice the associated overhead times. A viable workaround for unbinned readouts is currently available in the form of an alternate timing pattern which significantly reduces the crosstalk at the expense of a modest increase in readnoise and retains the nominal readout overhead time. The source of some of the crosstalk problem has been identified in the CEB and fixed in the non-flight electronics. The repair will be applied to the flight hardware at a future date; meanwhile, investigation into the camera detector head electronics are underway at the GSFC DCL in an effort to identify and remove any remaining sources of crosstalk.

Acknowledgements

Thanks are due to many team members who contributed to the crosstalk investigations, including E. Cheng, A. Waczynski, V. Argabright, T. Schoeneweis, S.Johnson, M. Troeltzsch, Y. Wen, T.Brown, H.Bushouse, K. Garcia, B. Greeley, D. Hickey, B.Hilbert, B. Hill, R. Kimble, J. Kirk, J. MacKenty, E. Malumuth, E. Polidan, W. Landsman, B. McLaughlin, O.Lupie, T.Pham, J.Pugliano, I.N. Reid, M.Robberto, A. Russell, S. Swain, and R. Telfer.

References

Janesick, James R., “Scientific Charge-Coupled Devices,” SPIE Press, Bellingham, WA, 2001.

Reid, I.Neill, “WFC3 Science Calibration, Summary assessment of December 2003/January 2004 science verification/calibration campaign,”, ISR 2004-02, Jan 22, 2004 (http://www.stsci.edu/hst/wfc3/documents/ISRs).

Appendix A

Summary of observations used in crosstalk investigations. Listed are the image identfication number, rootname, filename, aperture, filter, exposure time, amps used during the readout, gain setting, binning, and general comments.

ID	rootname	filename	aper	filter	expt	amps	gain	bin	comment
1573	IV070102	CSII03344151842_2	UVIS	F225W	200.0	ABCD	1.5	2	source in C, victim quad is D
1575	IV070104	CSII03344151842_4	UVIS	F606W	100.0	ABCD	1.5	2	source in C, victim quad is D
1577	IV070106	CSII03344151842_6	UVIS	F814W	50.0	ABCD	1.5	2	source in C, victim quad is D
1579	IV070108	CSII03344151842_8	UVIS	F814W	50.0	ABCD	1.5	2	source in A, victim quad is B
1581	IV07010A	CSII03344151842_10	UVIS	F606W	100.0	ABCD	1.5	2	source in A, victim quad is B
1587	IV07010G	CSII03344151842_16	UVIS	F606W	100.0	ABCD	1.5	2	
1589	IV07010J	CSII03344162014_1	UVIS	F814W	50.0	ABCD	1.5	2	
1593	IV07010N	CSII03344162014_5	UVIS	F606W	100.0	ABCD	1.5	2	
1841	IV02050V	CSII03346183252_13	UV14	F336W	10.0	ABCD	1.5	1	target barely saturated
1843	IV02050Y	CSII03346185127_1	UV14	F336W	100.0	ABCD	1.5	1	target barely saturated
1857	IV02051D	CSII03346192252_13	UV15	F606W	10.0	ABCD	1.5	1	target barely saturated
1873	IV02051V	CSII03346201433_13	UV16	F814W	10.0	ABCD	1.5	1	target barely saturated
2158	IV07040R	CSII03351194757_1	UV13	F300X	1.0	ABCD	1.0	2	
2159	IV07040S	CSII03351194757_2	UV13	F300X	100.0	ABCD	1.0	2	
2160	IV07040V	CSII03351195735_1	UV13	F300X	1.0	ABCD	1.5	2	
2161	IV07040W	CSII03351195735_2	UV13	F300X	100.0	ABCD	1.5	2	
2162	IV07040Y	CSII03351200713_1	UV13	F300X	1.0	ABCD	2.0	2	
2163	IV07040Z	CSII03351200713_2	UV13	F300X	100.0	ABCD	2.0	2	
2164	IV070411	CSII03351202402_1	UV13	F300X	1.0	ABCD	4.0	2	
2165	IV070412	CSII03351202402_2	UV13	F300X	100.0	ABCD	4.0	2	

ID	rootname	filename	aper	filter	expt	amps	gain	bin	comment
2554	IVA001OW	CSII03353175345_1	UVJ13	F625W	10.0	ABCD	1.5	1	unbinned
2555	IVA001OX	CSII03353181056_1	UVJ13	F625W	10.0	ABCD	1.5	2	
2556	IVA001OY	CSII03353182146_1	UVJ13	F625W	10.0	AD	1.5	1	
2557	IVA001OZ	CSII03353183435_1	UVJ13	F625W	10.0	BC	1.5	1	
2558	IVA001P0	CSII03353185020_1	UVJ13	F625W	10.0	AD	1.5	2	no apparent crosstalk
2559	IVA001P1	CSII03353185950_1	UVJ13	F625W	10.0	ABCD	1.5	3	
2560	IVA001P2	CSII03353191441_1	UVJ13	F625W	10.0	AD	1.5	3	no apparent crosstalk
2561	IVA001P3	CSII03353192426_1	UVJ13	F625W	10.0	AC	1.5	1	
2562	IVA001P4	CSII03353193445_1	UVJ13	F625W	10.0	BD	1.5	1	
2563	IVA001P5	CSII03353194648_1	UVJ13	F625W	10.0	BC	1.5	2	no apparent crosstalk
2564	IVA001P6	CSII03353195111_1	UVJ13	F625W	10.0	BC	1.5	3	no apparent crosstalk
2565	IVA001P7	CSII03353195543_1	UVJ13	F625W	10.0	AC	1.5	2	no apparent crosstalk
2566	IVA001P8	CSII03353200004_1	UVJ13	F625W	10.0	AC	1.5	3	no apparent crosstalk
2567	IVA001P9	CSII03353200438_1	UVJ13	F625W	10.0	BD	1.5	2	no apparent crosstalk
2568	IVA001PA	CSII03353200857_1	UVJ13	F625W	10.0	BD	1.5	3	no apparent crosstalk
2569	IVA001PB	CSII03353201855_1	UVJ13	F625W	10.0	ABCD	4.0	1	
2570	IVA001PC	CSII03353203423_1	UVJ13	F625W	10.0	ABCD	2.0	1	
2571	IVA001PD	CSII03353204334_1	UVJ13	F625W	10.0	ABCD	1.0	1	
2572	IVA001PE	CSII03353210634_1	UVJ13	F625W	10.0	ABCD	1.5	1	offset=3 (bias~2600 DN)
2573	IVA001PF	CSII03353212635_1	UVJ13	F625W	10.0	ABCD	1.5	1	offset=2 (bias~3300 DN)
2574	IVA001PG	CSII03353213603_1	UVJ13	F625W	10.0	ABCD	1.5	1	offset=1 (bias~4000 DN)
2575	IVA001PH	CSII03353214524_1	UVJ13	F625W	10.0	ABCD	1.5	1	offset=6 (bias~345 DN)
3315	IVA001SN	CSII04005204334_1	UVJ13	F625W	10.0	ABCD	1.5	1	baseline crosstalk image
3316	IVA001SO	CSII04005210014_1	UVJ13	F625W	10.0	ABCD	1.5	1	D amp gain = 4, others = 1.5
3317	IVA001SP	CSII04005211944_1	UVJ13	F625W	10.0	ABCD	1.5	1	D amp with offset of 3 (~2600DN; other amps at 0)
3318	IVA001SQ	CSII04005214310_1	UVJ14	F625W	10.0	ABCD	1.5	1	all amps gain=1.5
3319	IVA001SR	CSII04005220401_1	UVJ14	F625W	10.0	ABCD	2.0	1	A amp gain=2; other amps gain=1.5 source in B
3320	IVA001SS	CSII04006140734_1	UVJ14	F625W	10.0	ABCD	4.0	1	A amp gain=4, other amps gain=1.5 high backgrnd: laser diode on
3321	IVA001ST	CSII04006142714_1	UVJ14	F625W	10.0	ABCD	4.0	1	A amp gain=4; other amps gain=1.5
3322	IVA001SU	CSII04006144315_1	UVJ14	F625W	10.0	ABCD	1.5	1	all amps gain=1.5

ID	rootname	filename	aper	filter	expt	amps	gain	bin	comment
4093	IVA001SX	CSII04007170434_1	UVJ13	F625W	10.0	ABCD	1.5	1	baseline: target in D
4094	IVA001SY	CSII04007171904_1	UVJ13	F625W	10.0	ABCD	1.5	1	C amp gain=4.0; others 1.5; target in D
4095	IVA001SZ	CSII04007172850_1	UVJ13	F625W	10.0	ABCD	4.0	1	A amp gain=4.0; others 1.5; target in D
4096	IVA001T0	CSII04007174044_1	UVJ13	F625W	10.0	ABCD	1.5	1	bias offset=3 in A; target in D
4097	IVA001T1	CSII04007182030_1	UVJ13	F625W	10.0	ABCD	1.5	1	Tclamp=33µs; Tsample=8µs; serial shift=44µs
4098	IVA001T2	CSII04007183357_1	UVJ13	F625W	10.0	ABCD	1.5	1	Tclamp=33µs; Tsample=30µs; serial shift=66µs
4099	IVA001T3	CSII04007184717_1	UVJ13	F625W	10.0	ABCD	1.5	1	Tclamp=55µs; Tsample=8µs; serial shift=66µs
4100	IVA001T4	CSII04007185827_1	UVJ13	F625W	10.0	ABCD	1.5	1	Tclamp=22µs; Tsample=19µs; serial shift=44µs
4101	IVA001T5	CSII04007195203_1	UVJ13	F625W	10.0	ABCD	4.0	1	gain 4.0 in all quads; 4097 timing pattern.
4367	IVA001TC	CSII04014152534_1	UVJ16	F814W	10.0	ABCD	1.5	1	
4368	IVA001TD	CSII04014153949_1	UVJ13	F625W	10.0	ABCD	4.0	1	Initial timing pattern gain=4
4369	IVA001TE	CSII04014155006_1	UVJ13	F625W	10.0	ABCD	4.0	1	+1µs clamp high
4370	IVA001TF	CSII04014155931_1	UVJ13	F625W	10.0	ABCD	4.0	1	same as 4369
4371	IVA001TG	CSII04014160912_1	UVJ13	F625W	10.0	ABCD	4.0	1	+2µs clamp high
4372	IVA001TH	CSII04014161842_1	UVJ13	F625W	10.0	ABCD	4.0	1	+3µs clamp high
4373	IVA001TI	CSII04014162752_1	UVJ13	F625W	10.0	ABCD	4.0	1	+4µs clamp high
4374	IVA001TJ	CSII04014163738_1	UVJ13	F625W	10.0	ABCD	4.0	1	+5µs clamp high
4375	IVA001TK	CSII04014164646_1	UVJ13	F625W	10.0	ABCD	4.0	1	+6µs clamp high
4376	IVA001TL	CSII04014165638_1	UVJ13	F625W	10.0	ABCD	4.0	1	+7µs clamp high
4377	IVA001TM	CSII04014170600_1	UVJ13	F814W	1.0	ABCD	4.0	1	
4455	IVA001TN	CSII04014222504_1	UVJ13	F625W	1.0	ABCD	4.0	1	
4456	IVA001TO	CSII04014223849_1	UVJ13	F625W	10.0	ABCD	4.0	1	
4569	IVA001TQ	CSII04015221234_1	UVJ13	F625W	1.0	ABCD	4.0	1	
4570	IVA001TR	CSII04015222640_1	UVJ13	F625W	0.5	ABCD	4.0	1	
4665	IVA001TQ	CSII04020171830_1	UVJ13	F625W	10.0	ABCD	4.0	1	timing pattern -1 µs
4666	IVA001TR	CSII04020173253_1	UVJ13	F625W	10.0	ABCD	4.0	1	timing pattern -2 µs
4667	IVA001TS	CSII04020174531_1	UVJ13	F625W	10.0	ABCD	4.0	1	-3 µs
4668	IVA001TT	CSII04020175437_1	UVJ13	F625W	10.0	ABCD	4.0	1	-4 µs

ID	rootname	filename	aper	filter	expt	amps	gain	bin	comment
4906	IVA001U0	CSII04022221025_1	UVJ13	F625W	10.0	ABCD	1.5	1	-3 μs timing pattern; db=50
4907	IVA001U1	CSII04022222747_1	UVJ13	F625W	10.0	ABCD	1.5	1	-3 μs timing pattern; db=90
4908	IVA001U2	CSII04022224235_1	UVJ13	F625W	10.0	ABCD	1.5	1	-1 μs
4909	IVA001U3	CSII04022230206_1	UVJ13	F625W	10.0	ABCD	4.0	1	-3 μs timing pattern
4910	IVA001U4	CSII04023154247_1	UVJ13	F625W	10.0	ABCD	1.5	1	-4 μs clamp time timing pattern
4911	IVA001U5	CSII04023155624_1	UVJ13	F625W	10.0	ABCD	1.5	1	-2 μs
4912	IVA001U6	CSII04023161524_1	UVJ13	F625W	10.0	ABCD	1.5	1	nominal pattern (0 μs offset)
4913	IVA001U7	CSII04023163301_1	UVJ13	F625W	10.0	ABCD	1.5	1	+1 μs
4914	IVA001U8	CSII04023164427_1	UVJ13	F625W	10.0	ABCD	1.5	1	+2 μs
4915	IVA001U9	CSII04023165726_1	UVJ13	F625W	10.0	ABCD	1.5	1	+3 μs
4916	IVA001UA	CSII04023170728_1	UVJ13	F625W	10.0	ABCD	1.5	1	+4 μs
4917	IVA001UB	CSII04023171813_1	UVJ13	F625W	10.0	ABCD	1.5	1	+5 μs
4918	IVA001UC	CSII04023172851_1	UVJ13	F625W	10.0	ABCD	1.5	1	+7 μs
4919	IVA001UD	CSII04023175052_1	UVJ13	F625W	10.0	ABCD	1.5	1	-2 μs; unsaturated PSF
4920	IVA001UE	CSII04023181823_1	UVJ13	F625W	5.0	ABCD	1.5	1	-2 μs; un
4921	IVA001UF	CSII04023183238_1	UVJ13	F625W	20.0	ABCD	1.5	1	-2 μs; barely saturated PSF

Appendix B

Figure 9: Hard stretch (+/-3DN) showing the crosstalk reaction to small changes to the baseline 11μs clamp time, in gain=4 images. Shown are quadrant C crosstalk features only; in the absence of crosstalk, this quadrant would be blank. The upper row has the -4, -3, -2, -1μs offset clamp time patterns; middle row is 0, +1, +2, +3μs; lower row is +4, +5, +6, +7μs.